Theor. Appl. Climatol. 72, 209–220 (2002)

Theoretical and Applied Climatology

Department of Geophysics and Planetary Sciences, Faculty of Exact Sciences, Tel Aviv University, Israel

Decadal trends of main Eurasian oscillations and the Eastern Mediterranean precipitation

S. O. Krichak, P. Kishcha, and **P. Alpert**

With 8 Figures

Received April 5, 2001
Revised February 14, 2002

Summary

The role of the two main European low-frequency oscillations – the East Atlantic/West Russian (EA/WR) and the North Atlantic Oscillation (NAO), in controlling the precipitation in the Eastern Mediterranean region is investigated based on the NCEP/NCAR reanalysis and the Israeli precipitation data for 1958–1998. The data on the EA/WR and NAO indices, received from the NCEP Climate Prediction Center, are also adapted. Composite mean sea level and precipitation anomaly patterns are constructed and analyzed. In addition to the widely investigated positive NAO trend, another, also positive EA/WR trend characterized atmospheric developments during the period. During NAO positive months, the EA/WR-associated positive SLP anomaly areas were shifted from the east Atlantic to southwest Europe. The areas were shifted to the north during the NAO-negative months and were located over central and northern Europe. This demonstrates that the use of fixed pressure NAO patterns may be not the optimum way to understand climate variability. Analysis of the NAO, EA/WR patterns, as well as that of their decadal trends, demonstrated a relationship between the main European oscillations and the EM precipitation. The results allow explanation of the observed reduction of the north Israeli precipitation by the EA/WR positive trend during the period.

1. Introduction

The Eastern Mediterranean (EM) region is located in an area where both mid-latitude and equatorial atmospheric processes play significant roles during the rainy season. The role of the mid-latitude processes is evident (Petterssen, 1956; Reiter, 1975; Shay-El and Alpert, 1991; Shay-El et al., 2000; Illani, 1998). The role of the processes in the tropical Africa has been also demonstrated, e.g. Krishnamurti (1961); Krichak and Alpert (1998). The Red Sea Trough (RST) type circulation (Ashbel, 1938; Itzikson, 1997; Krichak et al., 1997a, b) is an impressive manifestation of the mid-latitude – equatorial area interactions in the Mediterranean region. Price et al. (1998) indicated a possible role of the El Nino associated effects.

The role of the North Atlantic Oscillation (NAO) in the European weather system has been widely investigated (e.g. Barnston and Livezey, 1987; Feldstein, 2000; Hurrell, 1995, 1996; Hurrell and van Loon, 1997; Latif, 1998; Latif et al., 1999; Ulbrich and Christoph, 1999; Ulbrich et al., 1999). The NAO is associated with the meridional oscillation in the Sea Level Pressure (SLP) with centers of action located in proximity to the Iceland low and Azores high. The last several decades were characterized by a positive NAO trend (Hurrell, 1995). Effects of the NAO trend over precipitation in Europe have been also analyzed (Hurrell, 1995; Hurrell and van Loon, 1997). Recently, Ben-Gai et al. (2001) demonstrated the existence of a high positive correlation between the height of the smoothed 1000 hPa over Israel and the NAO.

A high negative correlation between the NAO index and temperature variations in Israel was also detected. No role of the NAO in determining the EM precipitation was revealed in the study.

The role of another prominent European SLP anomaly system – the East Atlantic/West Russia (EA/WR) dipole pattern (Barnston and Livezey, 1987) – also appears to be important in the EM region. In winter, two main anomaly centers, located over the Caspian Sea and Western Europe, comprise the EA/WR. Positive phases of the pattern are characterized by the negative height anomalies throughout western and the southwestern Russia, and the positive height anomalies over north-western Europe. Negative phases of the pattern are associated with the positive height anomalies over the Caspian Sea and Western Russia and the negative height anomalies over north-western Europe. During the negative EA/WR phases, wetter than normal weather conditions are often observed over a large part of the Mediterranean region. Conversely, drier than normal conditions are often noted over a large part of the region during the EA/WR positive phases (Barnston and Livezey, 1987).

According to the gridded NASA reanalysis monthly means for 1980–1995, the extreme wet (dry) winter EM months were characterized by the anomaly patterns, that have much in common with those of the positive (negative) EA/WR phases (Krichak et al., 2000). Results by Benaroch (2000) and Kutiel and Benaroch (2001) also demonstrate a dependency of the EM precipitation on the characteristics of a dipole pattern with the centers located over the east Atlantic and the Caspian Sea areas.

The current analysis is focused on a further investigation of the role of main European atmospheric oscillations in the EM precipitation.

2. The data

41-year (1958–1998) gridded data from the National Center for Environmental Prediction/National Center for Atmospheric Research Reanalysis Project (NNRP) were used. The data were produced with the NNRP assimilation system based on the T62 (about 210 km) global spectral model. Results are available with 2.5 °lat × lon horizontal spacing (Kalnay et al., 1996; Kistler et al., 2001).

Composite SLP and precipitation anomaly patterns were computed for the wet and dry (above and below the 41-year means) December–February (DJF) months over the EM. The months were determined according to the NNRP precipitation intensity over a target area (33° N–36° N, 34° E–37° E) under an assumption that the target area represents the whole EM region. Additional composite patterns were also constructed for the positive and negative NAO and EA/WR months, based on the index values available from the NCEP Climate Prediction Center (CPC) website. The indices are determined according to the standard criteria (NAO – the pressure difference between the SLP values near Iceland and Azores; EA/WP – the pressure difference over E. Atlantic and north-Caspian regions).

3. Main SLP anomalies and the EM precipitation

The DJF anomaly patterns constructed for the positive NAO and EA/WR regimes are presented in Fig. 1a,b. The main typical features of the regimes are well represented here. A large negative SLP anomaly area is positioned over northwestern Europe during the positive NAO months (Fig. 1a). A positive SLP anomaly area is located over the Mediterranean region during such periods. A positive SLP anomaly zone occupies western Europe and the western part of the Mediterranean region during the positive EA/WR phase (Fig. 1b). An area with relatively low positive anomaly values was also found over the southern part of the EM region.

During the positive EA/WR periods (Fig. 1b), the EM weather processes are influenced by the negative SLP anomalies over the area, with the maximum over the Caspian region. A more intensive southward propagation of cold air masses from central Europe to the southern EM may be expected during such periods.

The corresponding precipitation anomaly patterns are presented in Fig. 2a,b. A similarity between the distributions of the precipitation maxima and those of the negative SLP anomalies may be observed. No indications of a dependency between the EM precipitation and the NAO index values were found. An area with

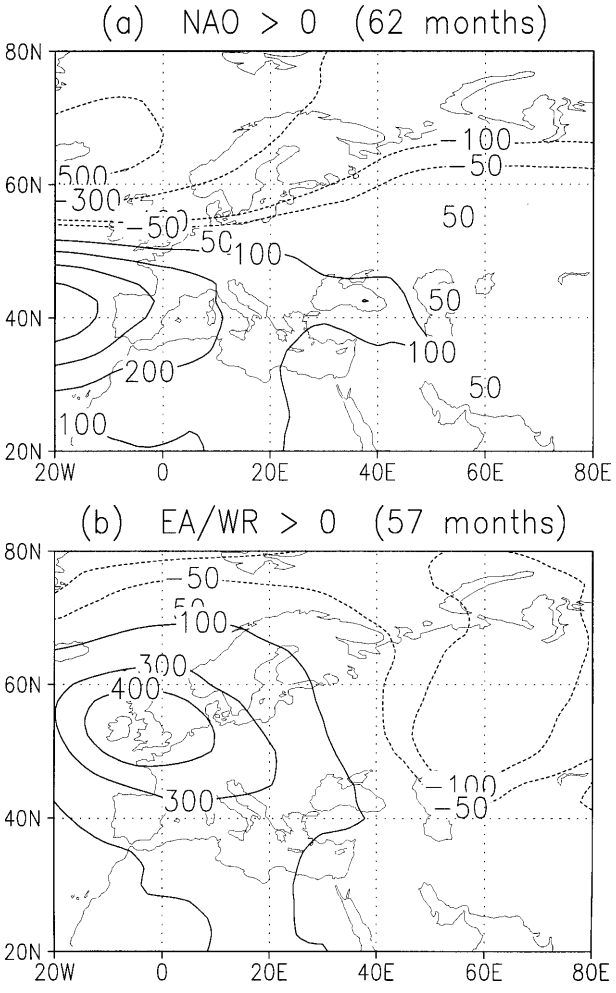

Fig. 1. Monthly mean DJF sea level pressure anomaly (current minus normal) patterns (Pa) for months with (**a**) NAO positive; (**b**) EA/WR positive

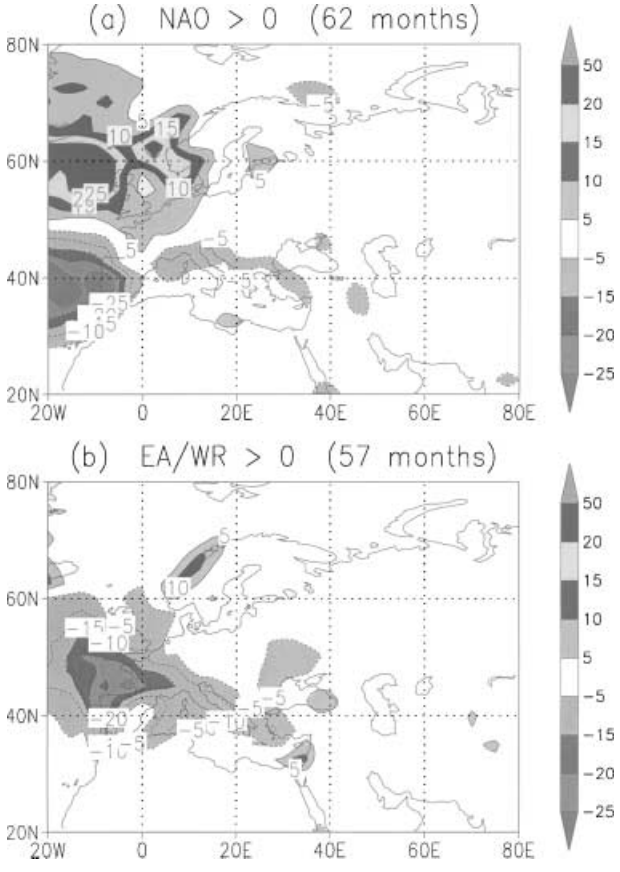

Fig. 2. Monthly mean DJF precipitation anomaly (current minus normal) patterns for months with different prominent anomaly patterns (mm): (**a**) NAO positive; (**b**) EA/WR positive

the positive precipitation anomaly ($\sim$5–10 mm/month) was found over the southern part of the EM (Fig. 2b), corresponding to the positive EA/WR phase. The positioning of the area indicates a positive dependency of the EM precipitation on the EA/WR.

The index values also provide information on the NAO and EA/WR trends over the last several decades. The numbers of months with different combinations of the NAO and EA/WR indices from 1958 to 1998 are presented in Table 1. The positive NAO trend (Hurrell, 1995) is well represented. Existence of an additional, also positive, EA/WR trend, may also be noted. An increase (9 cases in 1958–78; 20 cases in 1978–98) in the number of DJF months with both NAO and EA/WR indices positive, and a corresponding decrease in the number of DJF months with both indices negative (23 versus 7) may be indicated.

Composite SLP and precipitation anomaly patterns characterizing the months with the different combinations of NAO and EA/WR regimes are presented in Fig. 3a–d and Fig. 4a–d. Here the patterns on the left (right) side correspond to the periods with negative (positive) EA/WR regimes. Those on the top (bottom) of the figures are for the positive (negative) NAO regimes. The role of the NAO- and EA/WR-associated effects appears to be important for precipitation in the southern part of the EM. A comparison of the patterns in Fig. 2a and Fig. 4a demonstrates a similarity between the precipitation anomalies characterizing the pure NAO-negative and NAO–EA/WR-negative periods. The NAO–EA/WR positive conditions were associated with the wetter DJF months over the southern and the southeastern parts of the EM (Figs. 2b and 4b), rather than during the pure EA/WR positive

Table 1. Number of DJF months with different combinations of the SLP anomaly patterns over Europe

Years	NAO > 0	NAO < 0	EA/WR > 0	EA/WR < 0
1958–1978	25	36	20	38
1968–1988	30	31	29	29
1978–1998	38	24	35	23
Years	NAO > 0 EA/WR > 0	NAO > 0 EA/WR < 0	NAO < 0 EA/WR < 0	NAO < 0 EA/WR > 0
1958–1978	9	14	23	11
1968–1988	13	14	15	15
1978–1998	20	16	7	15

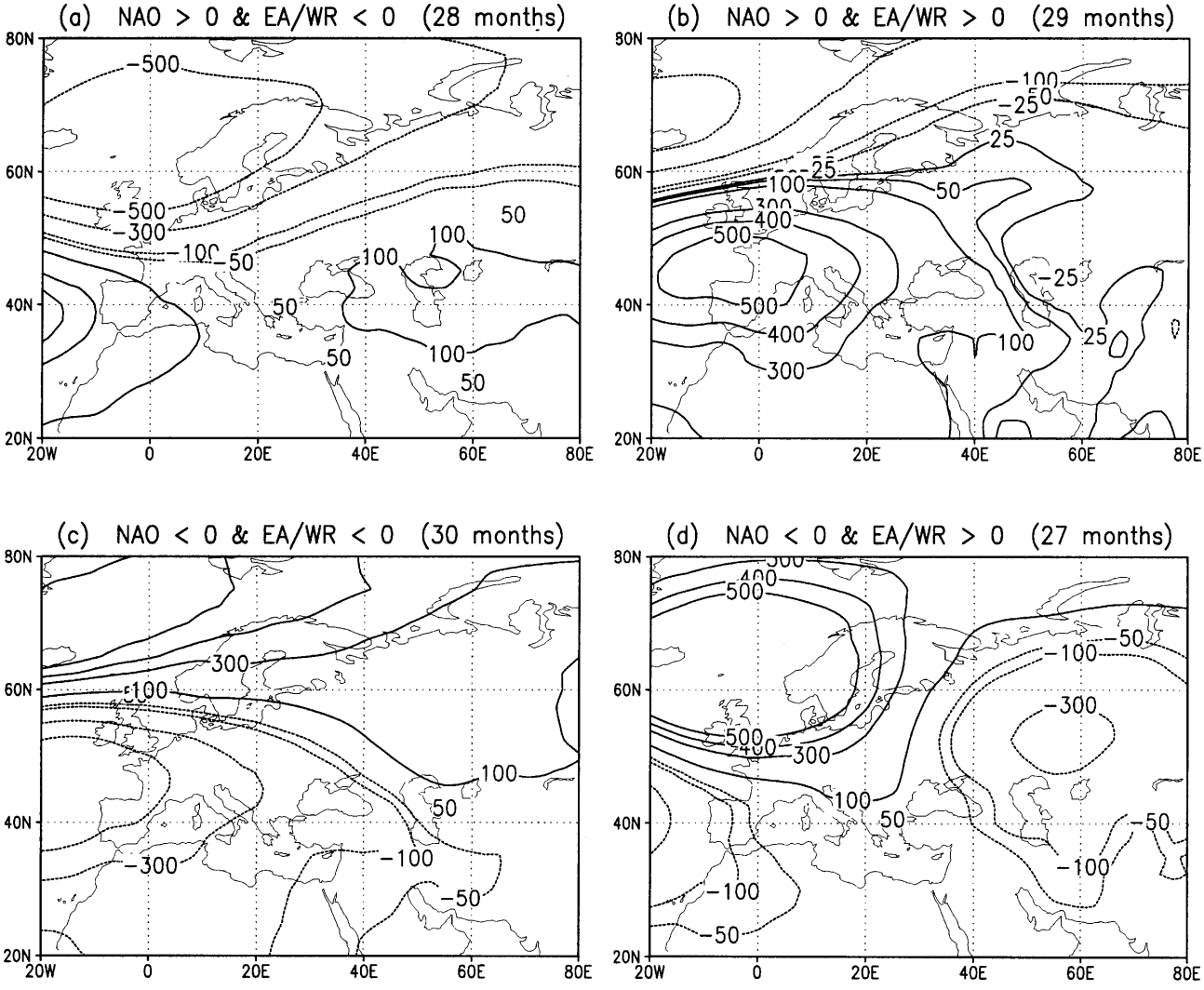

Fig. 3. Monthly mean DJF sea level pressure anomaly (current minus normal) patterns for months with jointly acting NAO and EA/WR anomaly patterns (Pa): (**a**) NAO positive, EA/WR negative; (**b**) NAO positive, EA/WR positive; (**c**) NAO negative, EA/WR negative EA/WR positive – bottom-right

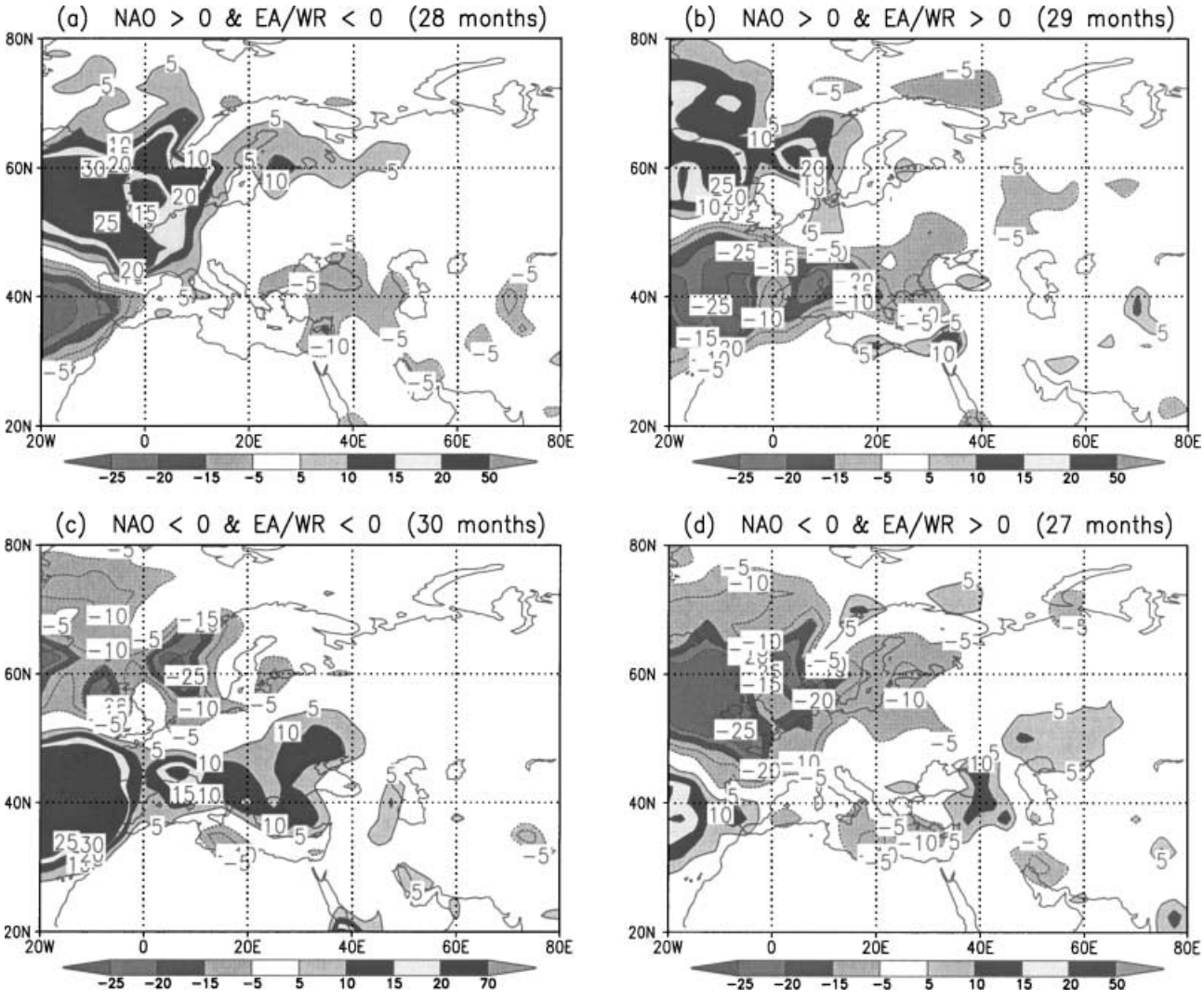

Fig. 4. Monthly mean DJF precipitation anomaly (current minus normal) patterns for months with jointly acting NAO and EA/WR anomaly patterns (mm): (**a**)–(**c**) as in Figs. 3

months. The periods were characterized by the negative precipitation anomaly over the northern and western parts of the Mediterranean region.

4. Decadal trends of wet/dry EM winter SLP anomaly patterns

The NNRP precipitation data allow constructing the SLP anomaly composites for the wet and dry months over the EM (Krichak et al., 2000). Such corresponding to the wetter-than-normal DJF months over the target area SLP anomaly pattern (Krichak et al., 2001a, b), is presented in Fig. 5. The pattern has much in common with patterns typical of the EA/WR positive regime (Fig. 1b). Analogously, the SLP anomaly pattern typical of the dry EM conditions (not presented) is similar

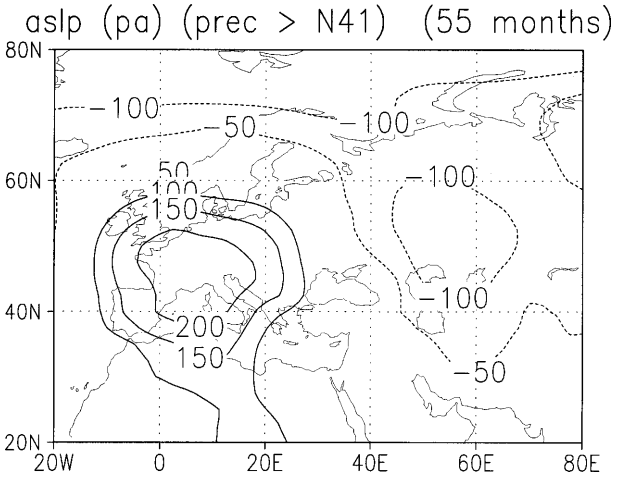

Fig. 5. Monthly mean DJF sea level pressure anomaly pattern (current minus normal) (hPa) with the EM precipitation anomaly more 100%

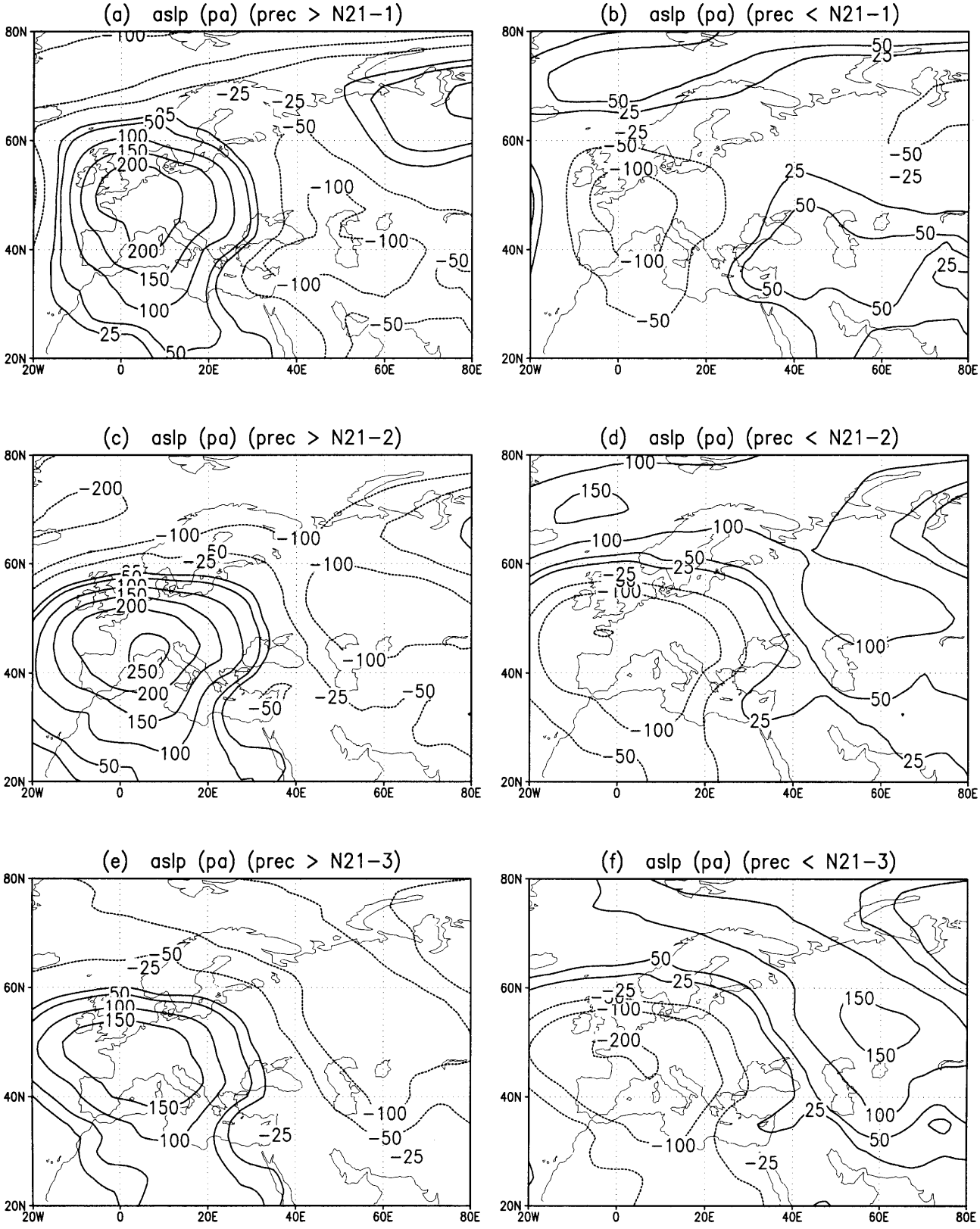

Fig. 6. Monthly mean sea level pressure anomaly patterns (current minus the corresponding normal) (Pa) for the periods with the wet and dry EM DJF for the three overlapping 21 y periods: Wet EM periods (**a**) 1958–1978; (**b**) 1968–1998; (**c**) 1978–1998. Dry EM periods (**d**) 1958–1978; (**e**) 1968–1998; (**f**) 1978–1998

to that of the negative EA/WR phase. The wet and dry EM associated patterns are not identical, however, to those of the positive and negative EA/WR periods. The positive anomaly center located over the west Europe (Fig. 5) is shifted, for instance to the southeast, compared to the corresponding center in Fig. 1b. The differences are evidently due to the role of other factors, that in addition to the EA/WR factors, in determining the EM precipitation regime.

The composite DJF SLP anomaly patterns characterizing the wet and dry EM DJF months, computed for three consecutive 21-year overlapping periods from 1958 to 1998 (Fig. 6a–f), are quite similar to those computed for the 41-year period. Patterns for the wet periods are given in Fig. 6a,c,e. The dry periods are represented by the patterns in Fig. 6b,d,f.

SLP anomaly patterns with EA/WR type dipoles are present in all the patterns. A long-term trend in positioning and intensity of the SLP anomaly dipole is noticeable. During 1958–78 the wet EM months were characterized by negative SLP anomaly over the EM region (Fig. 6a). The similar anomaly areas are also found in the Fig. 6c,e corresponding to 1968–88 and 1978–98, respectively. The areas are located, however, much further to the northeast. This indicates an increase of the relative importance of the positive SLP anomaly area over western Europe. Corresponding to the dry EM months patterns (Fig. 6b,d,f) illustrate an increase (of about 1.5–2.5 hPa) of the positive SLP anomaly over the area to the northeast of the Caspian Sea during the 40-year period. The positioning of the negative and positive SLP anomaly areas didn't change during the 1968–1998 period (Fig. 6d,f). This means that during the dry DJF months, the SLP anomaly trends were not contributing to the overall decrease of the EM precipitation (Ben-Gai et al., 1994).

5. EA/WR variations and precipitation in Israel

The discussed-above relationship between the EM precipitation and the characteristics of the large-scale European SLP anomalies was also found in the real data on precipitation in Israel (Kishcha et al., 2002). The following analysis is based on the data from three Israeli meteorological stations: Ayelet Hashahar (33.02° N, 35.57° E), Jerusalem (31.78° N, 35.22° E) and Beer Sheva (31.52° N, 34.80° E), representing here the northern, central and southern parts of the Israeli region respectively.

Observed DJF precipitation amounts normalized to the corresponding 41-year means are presented in Table 2, for eight combinations of the EA/WR and NAO indices. A similarity between the variations of precipitation amounts at all the stations may be noted. The variations are also in agreement with those of the NNRP-based precipitation estimates over the target area. The highest values of the EM precipitation anomalies characterized the periods with the positive EA/WR and NAO index values.

Table 2. DJF precipitation (in %) normalized to its 41-year mean for different combinations of the EA/WR and NAO indices

	NNRP target area	Ayelet	Jerusalem	Beer Sheva
Coordinates N	30–33 N	33.02 N	31.78 N	31.25 N
Coordinates E	33–37 E	35.57 E	35.22 E	34.80 E
Data source	NCEP data	Observ.	Observ.	Observ.
NAO > 0	102	102	110	107
NAO < 0	97	98	88	88
EAWR > 0	118	121	134	128
EAWR < 0	85	82	72	80
NAO > 0 & EAWR > 0	128	131	158	146
NAO < 0 & EAWR > 0	108	110	107	109
NAO < 0 & EAWR < 0	89	87	73	72
NAO > 0 & EAWR < 0	79	73	69	77

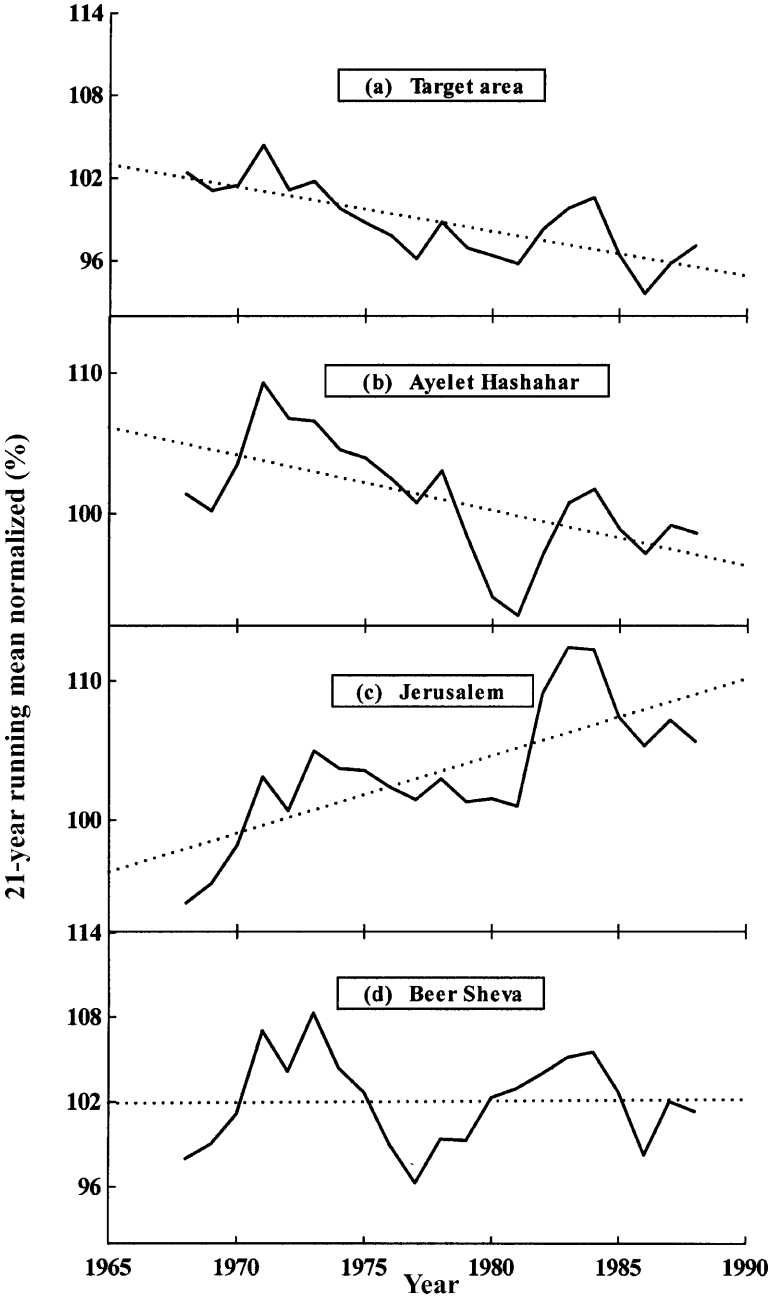

Fig. 7. Long-term variations of 21-year running mean of precipitation normalized to the 41-year mean (in %) for the target area and the three stations in Israel. (**a**) the target area; (**b**) Avelet Hashadar; (**c**) Jerusalem; (**d**) Beer Sheva. Dashed lines correspond to those of the linear regressions

A similarity between the time-variations of the 21-year running means of the normalized precipitation (NNRP data) over the target area (Fig. 7a) and those of the observations at the three stations (Fig. 7b,c,d) additionally illustrates the relationship. Differences were found between the precipitation trends in the three stations. A long-term decrease of the precipitation amount characterized the NNRP data as well as the observations at the Ayelet Hashahar (northern Israel). A long-term increase of precipitation was observed in Jerusalem with a tendency of about 0.55% per year. A weaker precipitation increase (0.011% per year) was also observed in Beer Sheva. These results are an agreement with Otterman et al. (1990), Steinberger and Gazit-Yaari (1996), Ben-Gai et al. (1994). The de-trended variations however are quite similar at all the four graphs.

Similarity between the four graphs in Fig. 7a–d is more evident in Fig. 8 presenting the curves of de-trended precipitation amounts at the locations. The precipitation variation in the Israeli part of the EM is associated with those of the EA/WR. The curve with the bold line in the

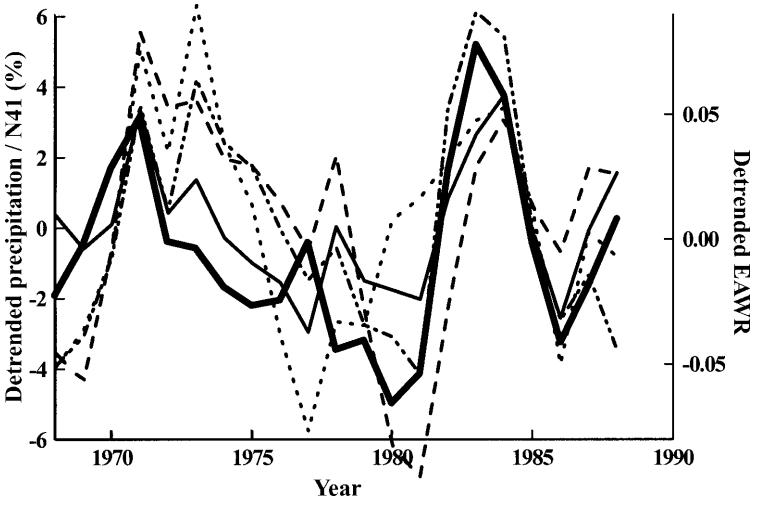

Fig. 8. Long-term variation of de-trended 21-year running means of precipitation (in %) at the three Israeli stations, over the target area and the EA/WR index. (bold line – EA/WR index; thin solid line – precipitation over the target area. dash, dash-dot and dotted lines are for Ayelet Hashahar, Jerusalem and Beer Sheva stations respectively)

figure represents de-trended EA/WR index variations. That with the thin solid line characterizes de-trended precipitation over the selected target area. The curves with the dash, dash-dot and dotted lines are for Ayelet Hashahar, Jerusalem and Beer Sheva stations respectively. The presented time variations at the stations and the target area similar to those of the de-trended EA/WR index values.

The relationship between the EA/WR de-trended index values ($\overline{EA}\,\overline{WR}$) and the observed precipitation was described by the following linear regression equation

$$\overline{P} = a + b \cdot \overline{EA}\,\overline{WR}$$

The linear dependencies are based on 21 pairs of the factors. The correlations obtained are presented in Table 3. The correlation equals 0.52 in northern Israel (Ayelet Hashahar), 0.71 in the central Israel (Jerusalem) and 0.48 in southern Israel (Beer Sheva). This indicates a dependency of the Israeli precipitation on the EA/WR variations. The results are statistically significant at the 95% level, according to the Fisher's test for small data sets (Wilks, 1995). As in the NNRP data, the highest EM precipitation amounts (de-trended) correspond to the periods with both the NAO and EA/WR positive.

Table 3. Correlation coefficients and parameters of the linear regression between de-trended precipitation $\overline{P}/\overline{P}_1$ and the de-trended EA/WR index

Equations	$\overline{P} = a + b \cdot \overline{EA}\,\overline{WR}$		
Parameter	r	a	b
NCEP target	0.79	0.223	38.839
Ayelet Hashahar	0.52	0.264	45.942
Jerusalem	0.71	0.338	60.724
Beer Sheva	0.48	0.222	40.438

6. Discussion and conclusions

The north European climate was significantly affected by the rise of the surface air temperature over the Northern Hemisphere during the 20th century (e.g. Shindell et al., 1999; Vinnikov et al., 2000). A notable (max. $\sim$3 hPa over N. Atlantic) SLP decrease took place between 1963–1993 over a large area over W. Europe to the north of 45–50° N. A DJF SLP increase (max. $\sim$2 hPa) has occurred (Latif, 2000) over Southern Europe and the Mediterranean area. The processes tended to intensify westerlies across the North Atlantic onto Europe, causing large-scale modulations of the normal patterns of the heat and moisture transport (Hurrell, 1995; Otterman et al., 1999). Deepening of the Iceland low as well as a consistent negative trend of the sea level pressure over the whole region during the last 25 years was registered (Latif et al., 1999; Hurrell, 1995).

The presented analysis demonstrates the existence of an additional trend in the European climate. The frequency of the positive EA/WR winter months has increased. Performed by Feldstein 2000, also a personal communication) analysis of the inter-annual properties of the EA/WR and NAO patterns from the perspective of climatic noise showed that the inter-annual variance of the both patterns exceeded the 95%

confidence level. The variance of the EA/WR patterns in fact only slightly exceeded the confidence level. The result allows conclusion that the NAO and EA/WR variations are in part driven by the processes in the hydrosphere or criosphere. The conclusion is more reliable in the case of NAO. The positive EA/WR trend during the last several decades may be associated with the positive NAO trend due to the strengthening of the both (i.e. also the southern) NAO centers of action (Paeth et al., 1999). The suggestion is also supported by results by Ulbrich and Christoph (1999) who analyzed the consequences of the eastward shift of the southern NAO positive center as simulated in several coupled atmosphere–ocean climate simulations with increased CO_2 concentration.

The process had important implications over the EM precipitation. During the negative EA/WR months, positive SLP anomaly areas were found to the northeast of the EM. Such periods were not favorable for the EM precipitation. Positions of both NAO-associated SLP anomaly centers during such months were quite similar to those of the standard NAO regime (Figs. 1a, 3a). The situation was different during the positive EA/WR periods, which were characterized by a different positioning of the NAO associated positive SLP anomaly centers during NAO positive and negative periods. During NAO positive months, the EA/WR-associated positive SLP anomaly areas were shifted from the east Atlantic to southwest Europe (Fig. 3b). The positive anomaly areas were shifted to the north during the NAO-negative months and were located over central and northern Europe (Fig. 3d).

Though relatively small, the displacements caused significant changes in the EM precipitation. Different precipitation anomaly conditions characterized EA/WR positive periods during NAO negative and positive regimes. During NAO negative periods, the area with positive precipitation anomaly was located to the northeast of the EM (Fig. 4d). The effect contributed to an increase in the precipitation intensity over the regions near the Caspian Sea. During NAO positive months, the area with the precipitation anomaly (max ~ 15 mm/month) was positioned over the southern part of the EM and Israel (Fig. 4b). The difference was evidently due a change in positioning of the EA/WR negative SLP anomaly areas (Fig. 3b,d). The frequency of realization of the EA/WR-positive–NAO-negative situations only slightly increased from 1958 to 1998 (Table 1). Such situations were favorable for the positive precipitation anomalies in the areas located to the northeast of the EM (Fig. 4d). The observed positive EA/WR trend was mainly associated with an increase in the number of the positive EA/WR–NAO situations (Table 1). The periods were characterized by the positive SLP anomalies over the southwest Europe and the north of the Mediterranean region (Fig. 3b), though no negative SLP anomaly area existed over the Caspian region (Fig. 3b). The situations were more favorable for a decrease in precipitation intensity in the EM (Fig. 4b). The observed negative trend of precipitation in northern Israel over the last decades was evidently associated with this effect. This demonstrates that the use of fixed pressure NAO patterns may be not the optimum way to understand climate variability effects in the EM.

The southern part of the EM was located in the area with a decreased intensity of positive SLP anomaly (Fig. 3b). The precipitation increase in this area during the NAO and EA/WR positive DJF months may be explained by a more active role of the mid-latitude-tropical area interactions in the region. The changes in the irrigation practices in Israel during the last several decades (Ben-Gai et al., 1993) could also be among the factors contributing to the observed precipitation increase.

The period of the analysis is too short for more definite conclusions. Further investigations, possibly including analyses of results of the global climate scenario simulations, are required. Still, the current results allow a new EM interpretation of the consequences of the observed decadal trends on the main European atmospheric oscillations.

Acknowledgements

NCAR-NCEP reanalysis data provided by the NOAA-CIRES Climate Diagnostic Center (CDC), Boulder, Colorado, USA, from their website at http://www.cdc.noaa.gov/ are used in the study. Multi-year series of the NAO and EA/WR index values have been obtained from the website of the NCEP Climate Prediction Center (CPC) at http://www.cpc.ncep.noaa/data/teledoc.

This research was supported by a grant (GLOWA) from Ministry of Science Culture and Sport, Israel and the

Bundesministerium für Bildung und Forschung (BMBF); Binational US-Israel Science Foundation (BSF) Grant No. 97-00448; EU Detect Project, and the Israeli Ministry of Science Grant No. 9470-98. Finally, we appreciate the constructive remarks and suggestions made by the reviewers.

References

Ashbel D (1938) Great floods in Sinai Peninsula, Palestine, Syria and the Syrian desert and the influence of the Red Sea on their formation. Quart J Meteor Soc 22: 635–639

Barston A, Livezey RE (1987) Classification, seasonality and persistence of low-frequency circulation patterns. Mon Wea Rev 115: 1083–1126

Benaroch Y (2000) Atmospheric teleconnections in the Mediterranean basin and the surrounding area. M.A. Thesis, Univ. of Haifa, 70 p

Ben-Gai T, Bitan A, Manes A, Alpert P (1993) Long term change in October rainfall patterns in southern Israel. Theor Appl Climatol 46: 209–217

Ben-Gai T, Bitan A, Manes A, Alpert P (1994) Long-term changes in annual rainfall patterns in southern Israel. Theor Appl Climatol 49: 67–59

Ben-Gai T, Bitan A, Manes A, Alpert P, Kushnir Y (2001) Temperature and Surface Pressure Anomalies in Israel and the North Atlantic Oscillation. Theor Appl Climatol 69: 171–177

Feldsten SB (2000) The timescale, power-spectra, and climate noise properties of teleconnection patterns. J Clim 13: 4430–4440

Hurrell JW (1995) Decadal Trends in the North Atlantic Oscillation: Regional Temperatures and Precipitation. Science 269: 676–679

Hurrell JW (1996) Influence of variations in extratropical wintertime teleconnections on Northern Hemisphere temperature. Geophys Res Lett 23(6): 665–668

Hurrell JW, van Loon H (1997) Decadal variations in climate associated with the North Atlantic Oscillation. Clim Change 36: 301–326

Ilani R (1998) Seasonal Forecast for Winter Precipitation in Israel Based on Principal Component Analysis. M.Sc Thesis, Dept. of Geophysics and Planetary Sci., Tel Aviv University, Tel Aviv, 120 p (in Hebrew)

Itzikson D (1995) Physical mechanisms of Tropical-Mid-Latitude interactions. M.Sc. Thesis, Dept. of Geophysics and Planetary Sci., Tel Aviv University (in Hebrew)

Kalnay E, Kanamitsu M, Kistler R, Collins W, Deaven D, Gandin L, Iredell M, Saha S, White G, Woolen J, Zhu Y, Chelliah M, Ebisuzaki W, Higgins W, Janowiak J, Mo KC, Ropelewsky C, Wang J, Leetma A, Reynolds R, Jenne R, Joseph D (1996) The NCEP/NCAR 40-Year Reanalysis Project. Bull Amer Meteor Soc 77: 437–471

Kishcha P, Krichak S, Alpert P (2002) Inter-Decadal Variations of Typical SLP Anomaly Patterns and Precipitation in Israel. Investigations of Ehuda and Shamron. V. 11, 287–300 (in Hebrew)

Kistler R, Collins W, Saha S, White G, Woolen J, Kalnay E, Chelliah M, Ebusisuzaki W, Kanamitsu M, Kousky V, van den Doll H, Jenke R, Fiorino M (2001) The NCEP-NCAR 50-year Reanalysis: Monthly Means CD-ROM and Documentation. Bull Amer Meteor Soc 82: 247–268

Krichak SO, Alpert P, Krishnamurti TN (1997a) Interaction of Topography and Tropospheric Flow – A Possible Generator for the Red Sea Trough? Meteorol Atmos Phys 63(3–4): 149–158

Krichak SO, Alpert P, Krishnamurti TN (1997b) Red Sea Trough/Cyclone Development – Numerical Investigation. Meteorol Atmos Phys 63(3–4): 159–170

Krichak SO, Alpert P (1998) Role of Large Scale Moist Dynamics in November 1–5 1994 Hazardous Mediterranean Weather. J Geoph Res 103(D16): 19,453–19,468

Krichak SO, Tsidulko M, Alpert P (1999) November 2 1994 Severe Storms in the Southeastern Mediterranean. Atmos Res 53: 45–62

Krichak SO, Tsidulko M, Alpert P (2000) Monthly Synoptic Patterns associated with wet/dry conditions in the Eastern Mediterranean. Theor Appl Climatol 65: 215–229

Krichak SO, Kishcha P, Alpert P (2001a) Low-frequency oscillation circulation patterns and precipitation in the eastern Mediterranean, OA 26.3 Climate Variability The northern oscillations: NAO and AO. European Geophysical Society XXVI General Assembly, Nice, France 25–30 March 2001

Krichak SO, Kishcha P, Alpert P (2001b) Decadal trends of NAO and EA/WR, SLP anomaly patterns and the Mediterranean precipitation. Abstracts of the Open Climate Conference August 20–24

Krishnamurti TN (1961) The sub-tropical jet stream of winter. J Meteorol 18: 172–191

Kutiel H, Benaroch Y (2002) North Sea-Caspian pattern (NCP) – an upper level atmospheric teleconnection affecting the Eastern Mediterranean: Identification and definition. Theor Appl Climatol 71: 17–28

Latif M (1998) Dynamics of interdecadal variability in coupled ocean–atmosphere models. J Climate 11: 602–624

Latif M, Timmerman A, Grotzner A, Eckert C, Voss R (1999) On North Atlantic Interdecadal Variability: A Stochastic view. Proc of the ECMWF seminar on Diagnosis of models and data assimilation systems, 6–10 Sept. 1999, March 2000, 139–172

Otterman J, Manes A, Rubin S, Alpert P, Starr DO'c (1990) An increase of early rains in southern Israel following land-use change. Bound-Layer Meteor 53: 333–351

Otterman J, Atlas R, Ardizzone J, Starr D, Jusem JS, Terry J (1999) Relationship of late-winter temperatures in Europe to North Atlantic surface winds: a correlation analysis. Theor Appl Climatol 64: 201–211

Paeth H, Hense A, Glowienska-Hense R, Voss R, Cubasch U (1999) The North Atlantic Oscillation as an indicator for greenhouse-gas indiced regional climate change. Clim Dynamics 15: 953–960

Petterssen S (1956) Weather analysis and forecasting, Vol 1. New York: McGraw-Hill Book Co., Inc., 428 p

Price C, Stone L, Rajagopalan B, Alpert P (1998) A possible link between El Nino and precipitation in Israel. Geophys Res Lett 25: 3963–3966

Shay-El Y, Alpert P (1991) A diagnostic study of winter diabatic heating in the Mediterranean in relation with cyclones. Quart J Roy Meteor Soc 117: 715–747

Shay-El Y, Alpert P, Da Silva A (2000) Preliminary estimation of horizontal fluxes of cloud liquid water in relation to subtropical moisture budget studies employing ISCCP, SSMI, and GEOS-1/DAS. J Geophys Res 105(D14): 18,067–18,089

Shindell DT, Miller RL, Schmidt GA, Pandolfo L (1999) Simulation of recent northern winter climate trends by greenhouse gas forcing. Nature 399: 452–455

Steinberger EH, Gazit-Yaari N (1996) Recent changes in the spatial distribution of annual precipitation in Israel. J Climate 9: 3328–3336

Ulbrich U, Christoph M (1999) A shift of the NAO and increasing storm track activity over Europe due to anthropogenic greenhouse gas forcing. Climate Dynamics 15: 551–559

Ulbrich U, Christoph M, Pinto JG, Corte-Real J (1999) Dependence of winter precipitation over Portugal on NAO and baroclinic wave activity. Int J Climatol 19: 379–390

Vinnikov KYa et al (1999) Global warming and Northern Hemisphere sea ice extent. Science 286: 1934–1937

Wilks HA (1995) Statistical methods in the atmospheric sciences: An introduction. Academic Press, 467 p

Author's address: Dr. Simon O. Krichak, Dept. of Geophysics and Planetary Sciences, Faculty of Exact Sciences, Tel Aviv University, Ramat Aviv, Tel Aviv, 69978, Israel (e-mail: shimon@cyclone.tau.ac.il).